RSC Advances




ROYAL SOCIETY OF CHEMISTRY

www.rsc.org/advances

Graphical Abstract:

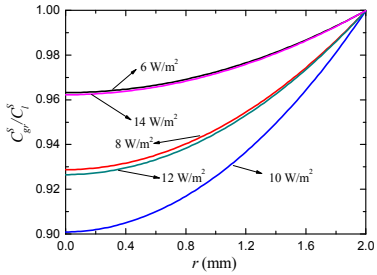


Substrate degradation and photo-hydrogen production under various light intensities was predicted using the developed two-phase mixture model.

RSC Advances

RSCPublishing

COMMUNICATION

# Two-phase mixture model for substrate degradation and photo-hydrogen production in the entrapped-cell photobioreactor under various light intensities

Cite this: DOI: 10.1039/x0xx00000x

Received ooth January 2012,
Accepted ooth January 2012

DOI: 10.1039/x0xx00000x

www.rsc.org/advances

Cheng-Long Guo,[*a] Hong-Xia Cao,[b] Hong-Shan Pei,[a] Fei-Qiang Guo[a] and Da-Meng Liu[cd]

**Two-phase mixture model was developed for revealing the interaction between substrate degradation and photo-hydrogen production in the entrapped-cell photobioreactor under various light intensities. The effects of the porosity of packed bed and the height of photobioreactor on substrate degradation rate (*SDR*) and hydrogen production rate (*HPR*) are also predicted at different light intensities.**

## 1. Introduction

Photosynthetic bacteria (PSB) is the most promising microorganism for biological hydrogen production because it not only possesses high theoretical conversion yield but also converses the light energy to produce hydrogen using simple organic compounds as hydrogen sources.[1-4] Currently, many studies on photo-hydrogen production are conducted using the cell immobilization techniques because of theirs advantages of the enhanced biomass retention and the improved stability.[5-8] Among these cell immobilization techniques, cell entrapped in porous gels is regarded as a more reasonable method due to the higher biomass content and local anaerobic environment created as well as the stably operation characteristic at a low hydraulic retention time.[9-11] Unfortunately, the entrapped-cell photobioreactor is still used in the stage of laboratory study owing to the lower photo-hydrogen production performance caused by the limitations of mass transfer and photo-biochemical reactions.[12] Therefore, the understanding with respect to the complicated mass transfer processes and photo-biochemical reactions is conducive to promote the applicability of the entrapped-cell photobioreactor in the bioconversion of organics for photo-hydrogen production. However, the experimentally measurements of the complex mass transfer processes and photo-biochemical reactions are very difficult to be performed due to the restriction of measuring instrument.

At present, it is interesting that the mass transfer processes and photo-biochemical reactions are investigated by the mathematical model as a powerful tool.[13-17] Moreover, photo-hydrogen production is usually predicted under various light intensities as one of the important factors affecting photo-biochemical reactions.[13, 18] Zhang et al utilized a two-dimensional mass transfer model to study the effects of light intensity on coupled processes of substrate transfer and degradation in an annular fiber-illuminating bioreactor.[13] Liao et al simulated the effect of light intensity on the flow and mass transfer process using lattice Boltzmann model coupled with a multi-block strategy.[14] In addition, it was also reported that the effect of light intensity on the glucose consumption efficiency and photo-hydrogen production rate was investigated using a one-dimensional two-phase flow and transport model.[15] However, to date, few models have focused on the interaction between substrate degradation and photo-hydrogen production under various light intensities.

In this work, two-phase mixture model is developed to predict photo-hydrogen production performance and substrate concentration distribution characteristics under various light intensities, and the numerical simulation results are validated using the experimental data reported by literature 11. In addition, the effects of the porosity of packed bed and the height of photobioreactor are also predicted at different light intensities.

## 2. Model development

The entrapped-cell photobioreactor was a working volume of $100\times40\times200$ mm$^3$ and packed with gel granules (4mm in diameter). The substrate flow direction in mainstream channel and the products transfer direction inside gel granule were defined as the *h*-direction and the *r*-direction, respectively. The illumination conditions were provided using LED lamps with main light wavelength of 590 nm,

[a] *School of Electric Power Engineering, China University of Mining and Technology, Xuzhou 221116, China. E-mail: clguo@cumt.edu.cn*
[b] *Low Carbon Energy Institute, China University of Mining and Technology, Xuzhou 221008, China.*
[c] *Guizhou Electric Power Test and Research Institute, Guiyang 550002, China.*
[d] *Institute of Engineering Thermophysics, Chongqing University, Chongqing 400030, China.*

where the operation temperature was set at 30 °C and the influent medium pH value was adjusted to 7.0. The glucose used as the sole carbon source was fed by a peristaltic pump, and then was degraded by the cells entrapped after being diffused into gel granules from mainstream channel. At last, the products were diffused out of gel granules followed by being discharged out of the entrapped-cell photobioreactor. Obviously, the photo-biochemical reactions as well as two-phase flow and mass transfer were present in the entrapped-cell photobioreactor. In this work, therefore, the assumptions were utilized to establish two-phase mixture model as following: (1) This work is performed at steady-state operating condition; (2) The substrate and products transfer processes in mainstream channel are one-dimensional flow along the *h*-direction; (3) Thermal physical properties of fluids are constant and the transfer processes can be described by Darcy's law; (4) The photo-biochemical reactions only occur inside gel granules; (5) The distribution and activity of PSB are uniform inside gel granules; (6) Hydrogen and carbon dioxide as the only gaseous products are generated by degrading glucose, and the mole ratio of them is 2:1 according to literature 19.

**Governing equations**

Mass conservation in liquid and gas phase as well as two-phase:[20, 21]

$$\nabla\cdot(\rho_{\mathrm{l}}\mathrm{u}_{\mathrm{l}})=\dot{m}_{\mathrm{l}} \tag{1}$$

$$\nabla\cdot(\rho_{\mathrm{g}}\mathrm{u}_{\mathrm{g}})=\dot{m}_{\mathrm{g}} \tag{2}$$

$$\nabla\cdot(\rho\mathrm{u})=\dot{m}_{\mathrm{l}}+\dot{m}_{\mathrm{g}} \tag{3}$$

where the subscript '$\mathrm{l}$' and '$\mathrm{g}$' refer to the liquid and gas phase, respectively. $\rho$ represents the density, kg/m$^3$; $\mathrm{u}$ the vector velocity, m/s; $\dot{m}$ the mass source, kg/m$^3$/s.

Momentum conservation in liquid and gas phase as well as two-phase:

$$\rho_{\mathrm{l}}\mathrm{u}_{\mathrm{l}}=-\frac{Kk_{\mathrm{rl}}}{v_{\mathrm{l}}}(\nabla p_{\mathrm{l}}-\rho_{\mathrm{l}}\mathrm{g}) \tag{4}$$

$$\rho_{\mathrm{g}}\mathrm{u}_{\mathrm{g}}=-\frac{Kk_{\mathrm{rg}}}{v_{\mathrm{g}}}(\nabla p_{\mathrm{g}}-\rho_{\mathrm{g}}\mathrm{g}) \tag{5}$$

$$\rho\mathrm{u}=-\frac{K}{v}\left(\nabla p-\gamma_{\rho}\rho\mathrm{g}\right) \tag{6}$$

where $k_{\mathrm{r}}$ is the relative permeability; $\mathrm{g}$ the gravitational acceleration, m/s$^2$. $K$ denotes the absolute permeability, m$^2$; $v$ the kinematic viscosity, m$^2$/s; $\gamma_{\rho}$ the density correlation factor, which can be given by:[22]

$$K=\frac{\varepsilon^3 d_{\mathrm{gr}}^2}{180(1-\varepsilon)^3} \tag{7}$$

$$v=\left(\frac{k_{\mathrm{rl}}}{v_{\mathrm{l}}}+\frac{k_{\mathrm{rg}}}{v_{\mathrm{g}}}\right)^{-1} \tag{8}$$

$$\gamma_{\rho}=\frac{\rho_{\mathrm{l}}\lambda_{\mathrm{l}}+\rho_{\mathrm{g}}\lambda_{\mathrm{g}}}{\rho_{\mathrm{l}}s_{\mathrm{l}}+\rho_{\mathrm{g}}s_{\mathrm{g}}} \tag{9}$$

where $\varepsilon$ is the porosity of packed bed; $d_{\mathrm{gr}}$ the diameter of gel granule, m; $s$ the saturation. Moreover, $\lambda$ denotes the mobility and can be calculated by:

$$\lambda_{\mathrm{l}}=\frac{k_{\mathrm{rl}}}{v_{\mathrm{l}}}v \tag{10}$$

$$\lambda_{\mathrm{g}}=\frac{k_{\mathrm{rg}}}{v_{\mathrm{g}}}v \tag{11}$$

$$\lambda_{\mathrm{l}}+\lambda_{\mathrm{g}}=1 \tag{12}$$

Substrate balance equation in the two-phase mixture:

$$\nabla\cdot\left(\varepsilon\rho D^{\mathrm{s}}\nabla\omega^{\mathrm{s}}\right)+\nabla\cdot\left\{\varepsilon\left[\rho_{\mathrm{l}}s_{\mathrm{l}}D_{\mathrm{l}}^{\mathrm{s}}\left(\nabla\omega_{\mathrm{l}}^{\mathrm{s}}-\nabla\omega^{\mathrm{s}}\right)+\rho_{\mathrm{g}}s_{\mathrm{g}}D_{\mathrm{g}}^{\mathrm{s}}\left(\nabla\omega_{\mathrm{g}}^{\mathrm{s}}-\nabla\omega^{\mathrm{s}}\right)\right]\right\}$$
$$-\nabla\cdot\left(\omega_{\mathrm{l}}^{\mathrm{s}}j_{\mathrm{l}}+\omega_{\mathrm{g}}^{\mathrm{s}}j_{\mathrm{g}}\right)-\phi^{\mathrm{s}}=\nabla\cdot\left(\gamma_{\mathrm{s}}\rho\mathrm{u}\omega^{\mathrm{s}}\right) \tag{13}$$

where the superscript '$\mathrm{s}$' refers to the substrate. $\phi^{\mathrm{s}}$ is the substrate degradation rate, kg/m$^3$/s; $\gamma_{\mathrm{s}}$ the advection correction factor; $\omega$ the mass fraction; $D$ the effective diffusion coefficient, m$^2$/s; $j$ the diffusive flux, kg/m$^2$/s; which can be calculated by:

$$\gamma_{\mathrm{s}}=\frac{\rho(\lambda_{\mathrm{l}}\omega_{\mathrm{l}}^{\mathrm{s}}+\lambda_{\mathrm{g}}\omega_{\mathrm{g}}^{\mathrm{s}})}{\rho_{\mathrm{l}}s_{\mathrm{l}}\omega_{\mathrm{l}}^{\mathrm{s}}+\rho_{\mathrm{g}}s_{\mathrm{g}}\omega_{\mathrm{g}}^{\mathrm{s}}} \tag{14}$$

$$\rho\omega^{\mathrm{s}}=\rho_{\mathrm{l}}s_{\mathrm{l}}\omega_{\mathrm{l}}^{\mathrm{s}}+\rho_{\mathrm{g}}s_{\mathrm{g}}\omega_{\mathrm{g}}^{\mathrm{s}} \tag{15}$$

$$\rho D^{\mathrm{s}}=\rho_{\mathrm{l}}s_{\mathrm{l}}D_{\mathrm{l}}^{\mathrm{s}}+\rho_{\mathrm{g}}s_{\mathrm{g}}D_{\mathrm{g}}^{\mathrm{s}} \tag{16}$$

$$j_{\mathrm{l}}=\frac{\lambda_{\mathrm{l}}\lambda_{\mathrm{g}}K}{v}\left[\nabla P_c+\left(\rho_{\mathrm{l}}-\rho_{\mathrm{g}}\right)\mathrm{g}\right] \tag{17}$$

$$j_{\mathrm{l}}+j_{\mathrm{g}}=0 \tag{18}$$

In addition, the relative permeability of gas and liquid phase as well as the capillary pressure can be given by:[23, 24]

$$k_{\mathrm{rl}}=s_{\mathrm{l}}^3 \tag{19}$$

$$k_{\mathrm{rg}}=(1-s_{\mathrm{l}})^3 \tag{20}$$

$$p_{\mathrm{c}}=p_{\mathrm{g}}-p_{\mathrm{l}}=\sigma(\frac{\varepsilon}{K})^{\frac{1}{2}}J(s_{\mathrm{l}}) \tag{21}$$

where $\sigma$ is the liquid-gas interfacial tension, N/m. The Leverett function $J(s_{\mathrm{l}})$ can be calculated by:[25]

$$J\left(s_{\mathrm{l}}\right)=1.417\left(1-s_{\mathrm{l}}\right)-2.12\left(1-s_{\mathrm{l}}\right)^2+1.263\left(1-s_{\mathrm{l}}\right)^3 \tag{22}$$

The substrate transfer in gas phase can be neglected. That is,

$$\omega_{\mathrm{g}}^{\mathrm{s}}=0,\quad D_{\mathrm{g}}^{\mathrm{s}}=0 \tag{23}$$

The local substrate concentration in the two-phase mixture and liquid phase are defined by:

$$C^{\mathrm{s}}=\rho\omega^{\mathrm{s}}=s_{\mathrm{l}}C_{\mathrm{l}}^{\mathrm{s}}=s_{\mathrm{l}}\rho_{\mathrm{l}}\omega_{\mathrm{l}}^{\mathrm{s}} \tag{24}$$

The boundary conditions can be obtained as following:

At the inlet of the entrapped-cell photobioreactor:

$$C^{\mathrm{s}}=C_{\mathrm{in}}^{\mathrm{s}},\quad s_{\mathrm{l}}=1 \tag{25}$$

$$\rho_{\mathrm{l}}\mathrm{u}_{\mathrm{l}}=\rho_{\mathrm{l}}\mathrm{u}_{\mathrm{l,\,in}},\quad \rho_{\mathrm{g}}\mathrm{u}_{\mathrm{g}}=0 \tag{26}$$

At the outlet of the entrapped-cell photobioreactor:

$$\frac{dC^{\mathrm{s}}}{dh}=0 \tag{27}$$

**Mass transfer inside gel granule**

The substrate transfer is dominated by diffusion inside gel granule and the substrate transfer processes can be modelled by Fick's law. Therefore, it can be obtained as following:[26, 27]

$$D_{\mathrm{gr}}^{\mathrm{s}}\frac{d^2C_{\mathrm{gr}}^{\mathrm{s}}}{dr^2}+\frac{2D_{\mathrm{gr}}^{\mathrm{s}}}{r}\frac{dC_{\mathrm{gr}}^{\mathrm{s}}}{dr}=\frac{\psi C^{\mathrm{c}}}{M^{\mathrm{s}}}(\frac{1}{Y_{\mathrm{x/s}}}\mu+m) \tag{28}$$

where the subscript '$\mathrm{gr}$' refers to the gel granule. $Y_{\mathrm{x/s}}$ is the cell yield; $\psi$ the cell density increasing coefficient; $C^{\mathrm{c}}$ the cell density, kg/m$^3$; $M$ is the molecular weight, kg/mol; $\mu$ and $m$ denote the

specific growth rate and maintenance coefficient, respectively, and can be described by:[15, 16]

$$m = 0.562137\exp\left(-2.8\left(I_0^{1.031}/10.8-1\right)^2\right) \quad (29)$$

$$\mu = \mu_{\max}\frac{C_{gr}^{s}}{K_s + C_{gr}^{s}} \quad (30)$$

where $I_0$ denote the light intensity, W/m$^2$; $K_s$ the Monod constant, mM. $\mu_{\max}$ is the maximum specific growth rate and can be calculated by:[15, 16]

$$\mu_{\max} = 0.25986\exp\left(-1.2\left(I_0^{1.031}/10.8-1\right)^2\right) \quad (31)$$

The corresponding boundary conditions can be obtained as:

$$r = 0, \qquad \frac{dC_{gr}^{s}}{dr} = 0 \quad (32)$$

$$r = \mathrm{R}, \qquad C_{gr}^{s} = C_l^{s} \quad (33)$$

The mass transfer of hydrogen produced is also dominated by diffusion in gel granule, which can be expressed by Fick's law and Luedeking-Piret model:[27, 28]

$$D_{gr}^{H_2}\frac{d^2C_{gr}^{H_2}}{dr^2} + \frac{2D_{gr}^{H_2}}{r}\frac{dC_{gr}^{H_2}}{dr} = \frac{\psi C^{c}}{M^{H_2}}(\alpha^{*}\frac{1}{Y_{x/s}}\mu + \beta) \quad (34)$$

where the superscript '$H_2$' refers to the hydrogen produced. $\beta$ is the growth associated kinetic constant, 1/s. $\alpha^*$ denotes the non-growth associated kinetic constant and can be calculated by:[15]

$$\alpha^{*} = 0.0192\exp\left(-9.5\left(I_0^{1.031}/10.8-1\right)^2\right) \quad (35)$$

The corresponding boundary conditions can be obtained as:

$$r = 0, \qquad \frac{dC_{gr}^{H_2}}{dr} = 0 \quad (36)$$

$$r = \mathrm{R}, \qquad C_{gr}^{H_2} = C_g^{H_2} \quad (37)$$

Therefore, the substrate degradation rate $\phi^{s}$ and the hydrogen production rate $\phi^{H_2}$ can be given by:

$$\phi^{s} = \alpha M^{s} D_{gr}^{s}\left.\frac{dC_{gr}^{s}}{dr}\right|_{r=\mathrm{R}} \quad (38)$$

$$\phi^{H_2} = \alpha M^{H_2} D_{gr}^{H_2}\left.\frac{dC_{gr}^{H_2}}{dr}\right|_{r=\mathrm{R}} \quad (39)$$

where $\alpha$ is the specific area of gel granules in the elemental volume, 1/m.

Moreover, the interfacial mass transfer rate of gas and liquid phase can be expressed as:

$$\dot{m}_l = -\phi^{s} \quad (40)$$

$$\dot{m}_g = \phi^{H_2} + \phi^{CO_2} \quad (41)$$

where the superscript '$CO_2$' refers to the carbon dioxide produced.

The hydrogen production rate $\phi^{H_2}$ and the carbon dioxide production rate $\phi^{CO_2}$ can be calculated by:

$$2\phi^{CO_2}/M^{CO_2} = \phi^{H_2}/M^{H_2} \quad (42)$$

**Estimation of photo-hydrogen production**

Substrate degradation and photo-hydrogen production in the entrapped-cell photobioreactor were assessed by substrate degradation rate (*SDR*) and hydrogen production rate (*HPR*), which can be defined as: [5, 15]

$$SDR\ (\mathrm{mmol/L/h}) = \frac{\Delta CSD\ (\mathrm{mmol})}{\Delta T\ (\mathrm{h}) \times \text{Photobioreactor volume (L)}} \quad (43)$$

$$HPR\ (\mathrm{mmol/L/h}) = \frac{\Delta CHP\ (\mathrm{mmol})}{\Delta T\ (\mathrm{h}) \times \text{Photobioreactor volume (L)}} \quad (44)$$

where $\Delta T$ is the hydrogen evolution time, $\Delta CSD$ and $\Delta CHP$ represent the increments of cumulative substrate degradation and hydrogen production, respectively.

**Numerical simulation procedure**

The self-written code in FORTRAN language based on the Gauss-Seidel algorithm was used to iteratively solve the above governing equations described by finite volume method.[29] Moreover, the independent of the simulation results and the grid size was ensured by performing the rigorous numerical tests. The model mentioned above was validated against the experimental data obtained from literature 11. In addition, as shown in Table 1, the photo-biochemical and thermal physical properties were used to predict photo-hydrogen production performance and substrate concentration distribution characteristics.[11, 15, 26]

**Table 1** Parameters used in the model

| Parameter | value | Parameter | value |
|---|---|---|---|
| $C^{c}$ (kg/m$^3$) | 0.76 | $\alpha$ (1/m) | 930 |
| $C_g^{H_2}$ (mM) | 29.76 | $\beta$ (1/h) | $1.5\times10^{-3}$ |
| $C_{in}^{s}$ (mM) | 60 | $\varepsilon$ | 0.38 |
| $D_{gr}^{H_2}$ (m$^2$/h) | $2.29\times10^{-6}$ | $v_g$ (m$^3$/h) | 0.356 |
| $D_{gr}^{s}$ (m$^2$/h) | $2.86\times10^{-6}$ | $v_l$ (m$^3$/h) | $2.88\times10^{-3}$ |
| $D_l^{s}$ (m$^2$/h) | $6.06\times10^{-6}$ | $\rho_g$ (kg/m$^3$) | 0.714 |
| $K_s$ (mM) | 28.9 | $\sigma$ (N/m) | $7.28\times10^{-2}$ |
| $Y_{x/s}$ | 0.61 | $\psi$ | 1.97 |

## 3. Results and discussion

**Effect of light intensity**

The light intensity is a critical factor affecting photo-biochemical reactions because of the sensitivity of photosynthetic system to light intensity.[11] Suitable light intensity contributes to maximize photo-hydrogen production performance by the enhancement of the PSB's activity. In this work, the effects of light intensities from 6 to 14 W/m$^2$ on substrate degradation and photo-hydrogen production were predicted to determine the optimal light intensity for the maximum *SDR* and *HPR* yielded in the entrapped-cell photobioreactor.

As shown in Fig.1, the numerical simulation results are given for comparison with the experimental data under various light intensities obtained from litter 11. The relative deviations between the numerical simulation results and the experimental data are within the range of -8.6~+2.8 % and -29.2~ +23.6 % for the *SDR* and the *HPR*, respectively. Obviously, the *SDR* and the *HPR* firstly improved with the increase of light intensity because the amount of electrons and ATP stimulated were gradually sufficient with the enhancement of the photons captured by the photosynthetic apparatus of the PSB. However, the *SDR* and the *HPR* dropped when the light intensity further increased beyond the critical threshold. It can be attributed to the fact that the higher light intensity results in a photo-inhibition phenomenon because the excessive photons

captured converts into overfull heat energy to damage the photosynthetic apparatus of the PSB.[30] Hence, the proper light intensity maintained is critically significant for the improvement on photo-hydrogen production performance of the entrapped-cell photobioreactor.

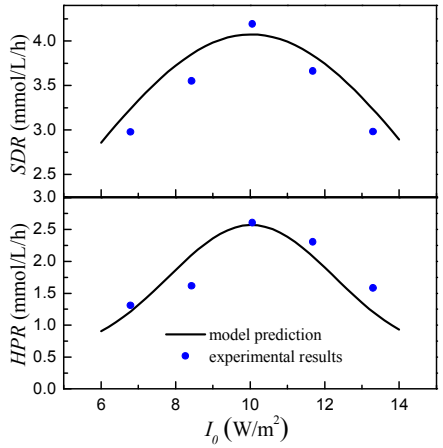


**Fig.1** Effect of light intensity on the *SDR* and the *HPR*

For understanding the influence of light intensity on substrate concentration distribution characteristics, as shown in Fig.2, the $C_l^s$ and $C_{gr}^s/C_l^s$ are predicted under five light intensities (6, 8, 10, 12 and 14 W/m$^2$). It can be seen that, at a specific light intensity, the substrate concentrations decrease along the *h*-direction and the reverse *r*-direction due to the substrate degraded by photo-biochemical reactions. Under the light intensity of 10 W/m$^2$, the lowest substrate concentrations were achieved at the outlet of the entrapped-cell photobioreactor and the surface of gel granule, which indicates that the substrate degradation performance is a maximum. These results coincide with the variation trend of the *SDR* mentioned above (cf. Fig.1).

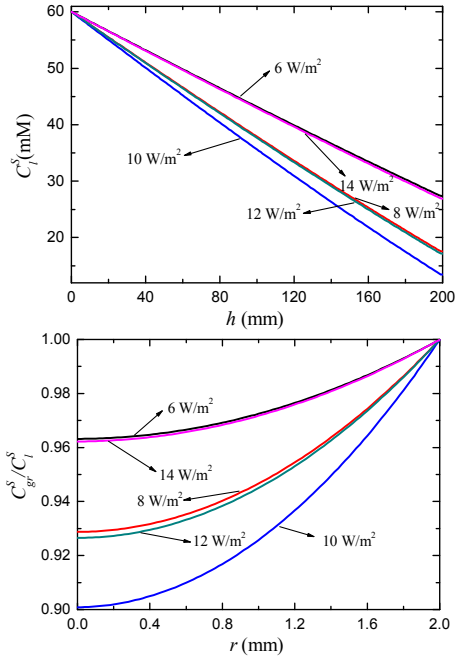


**Fig.2** Effect of light intensity on $C_l^s$ and $C_{gr}^s/C_l^s$.

**Effect of the porosity of packed bed**

A variation of the porosity of packed bed can result in a change of the mass transfer processes of substrate and products because it can significantly affect the specific area of gel granules in the elemental volume. In this work, therefore, the effect of the porosity of packed bed on substrate degradation and photo-hydrogen production of the entrapped-cell photobioreactor is investigated under various light intensities and the numerical simulation results are shown in Fig.3.

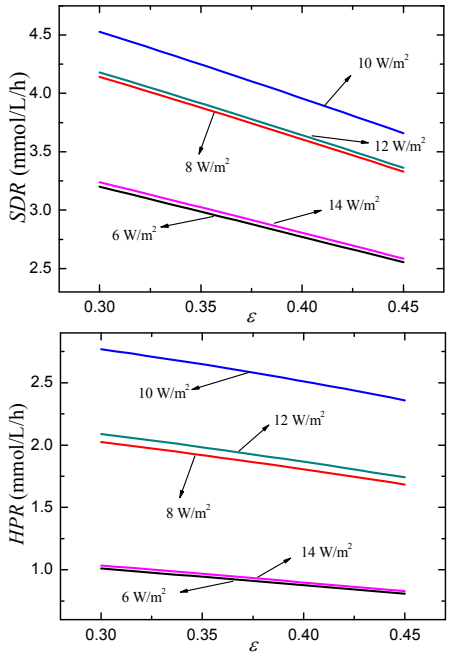


**Fig. 3** Effect of the porosity of packed bed on the *SDR*s and the *HPR*s under various light intensities

It can be seen that the *SDR*s decreased monotonically with increasing the porosity of packed bed from 0.30 to 0.45, while the *HPR*s also dropped monotonically. It can be explained by the fact that the increase of the porosity of packed bed leads to the decrease in the specific area of gel granules in the elemental volume, lowering the amount of substrate transferred into gel granules and subsequently negatively affecting the photo-hydrogen production performance of the entrapped-cell photobioreactor. Based on these results obtained, it can be summarized that a higher porosity of packed bed is beneficial to the improvement on photo-hydrogen production performance of the entrapped-cell photobioreactor.

**Effect of the height of photobioreactor**

It is known that the height of photobioreactor is one of key factors affecting substrate degradation and photo-hydrogen production in the entrapped-cell photobioreactor. In this section, therefore, the *SDR*s and *HPR*s were studied under different heights of photobioreactor by two-phase mixture model, and the porosity of packed bed was set at 0.38.

Fig.4 shows the effect of the height of photobioreactor on the *SDR*s and the *HPR*s under various light intensities. It can be seen that the *SDR*s and the *HPR*s decrease monotonically with the increase of the height of photobioreactor from 150 to 250 mm. This behaviour can be explained by that the continuous substrate degradation for producing hydrogen gradually

exacerbates the insufficient substrate supplied for PSB as the increased height of photobioreactor, lowering the performance of substrate degradation and photo-hydrogen production. Moreover, for a given height of photobioreactor, it can be found that both too high and too low light intensity result in the poor *SDR*s and the lower *HPR*s, and the highest *SDR* and *HPR* were achieved at the light intensity of 10 W/m$^2$ because the combined effect of the effective absorption of light energy and the photo-inhibition of photosynthesis.

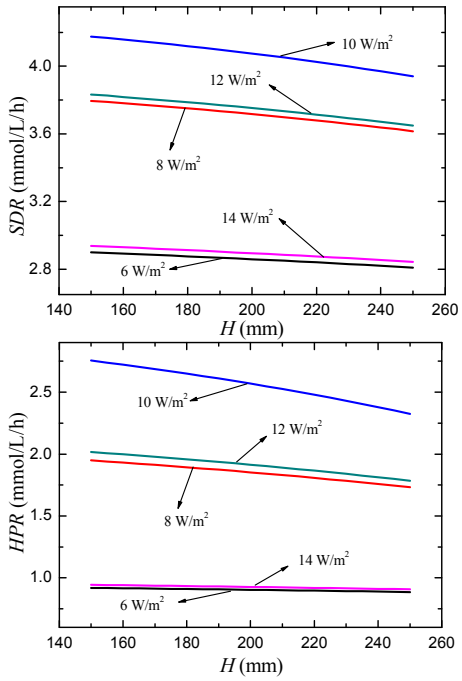


**Fig. 4** Effect of the height of photobioreactor on the *SDR*s and the *HPR*s under various light intensities

## Conclusions

In this work, two-phase mixture model has been established to predict substrate degradation and photo-hydrogen production in the entrapped-cell photobioreactor under various light intensities based on photo-biochemical reaction kinetics and mass transfer principles. The main conclusions are summarized as follows:

(1) The predicted results of the substrate degradation rate (*SDR*) and hydrogen production rate (*HPR*) agree well with the reported experimental data under various light intensities.

(2) The most suitable condition for substrate degradation to produce hydrogen was at the light intensity of 10 W/m$^2$.

(3) The increases of the porosity of packed bed and the height of photobioreactor lowered photo-hydrogen production performance of the entrapped-cell photobioreactor.

## Acknowledgements

The authors gratefully acknowledge financial supported by the National Natural Science Foundation of China (No. 51406227) and the Fundamental Research Funds for the Central Universities (No. 2014QNB03).

## References

1 H. Y. Ren, B. F. Liu, J. Ding, G. J. Xie, L. Zhao, D. F. Xing and N. Q. Ren, *RSC Adv*, 2012, **2**(13), 5531-5535.
2 M. D. Redwood, R. L. Orozco, A. J. Majewski and L. E. Macaskie, *Bioresourc Technol*, 2012, **119**, 384-392.
3 N. Basak, A. K. Jana, D. Das and D. Saikia, *Int J Hydrogen Energ*, 2014, **39**(13), 6853-6871.
4 J. Cai and G. Wang, *Bioresourc Technol*, 2014, **154**, 254-259.
5 C. L. Guo, X. Zhu, Q. Liao, Y. Z. Wang, R. Chen and D. J. Lee, *Bioresourc Technol*, 2011, **102**(18), 8507-8513.
6 H. Y. Ren, B. F. Liu, G. J. Xie, L. Zhao and N. Q. Ren, *GCB Bioenergy*, 2013, **6**, 599-605.
7 G. J. Xie, B. F. Liu, D. F. Xing, J. Nan, J. Ding, H. Y. Ren and N. Q. Ren, *RSC Adv*, 2012, **2**(6), 2225-2228.
8 C. L. Guo, H. X. Cao, F. Q. Guo, C. L. Huang, H. G. Wang and Z. H. Rao, *Biotechnol Lett*, 2014, DOI 10.1007/s10529-014-1677-0.
9 Y. Z. Wang, Q. Liao, X. Zhu, R. Chen, C. L. Guo and J. Zhou, *Bioresourc Technol*, 2013, **135**, 331-338.
10 X. Tian, Q. Liao, W. Liu, Y. Z. Wang, X. Zhu, J. Li and H. Wang, *Int J Hydrogen Energ*, 2009, **11**, 4708-4717.
11 Y. Z. Wang, Q. Liao, X. Zhu, X. Tian and C. Zhang, *Bioresourc Technol*, 2010, **101**(11), 4034-4041.
12 M. Y. Azwar, M. A. Hussain and A. K. Abdul-Wahab, *Renew Sust Energ Rev*, 2014, **31**, 158-173.
13 C. Zhang, H. Zhang, Z. Zhang, Y. Jiao and Q. Zhang, *J Photoch Photobio B*, 2014, **131**, 113-119.
14 Q. Liao, Y. X. Yang, X. Zhu and R. Chen, *J Hydrogen Energ*, 2013, **38**(35), 15700-15709.
15 Q. Liao, D. M. Liu, D. D. Ye, X. Zhu and D. J. Lee, *J Hydrogen Energ*, 2011, **36**(21), 13939-13948.
16 R. Chen, Y. K. Pu, Q. Liao, X. Zhu and Y. Z. Wang, *J Hydrogen Energ*, 2013, **38**(35), 15670-15679.
17 C. Zhang, A. J. Wang and Q. G. Zhang, *Biotechnol Lett*, 2013, **35**(10), 1579-1587.
18 H. Argun and F. Kargi, *J Hydrogen Energ*, 2010, **4**, 1595-1603.
19 H. Koku, I. Eroğlu, U. Gündüz, M. Yücel and L. Türker, *J Hydrogen Energ*, 2002, **27**(11), 1315-1329.
20 C. Y. Wang and C. Beckermann, *Int J Heat Mass Tran*, 1993, **36**, 2747-2747.
21 C. Y. Wang and P. Cheng, *Int J Heat Mass Tran*, 1996, **39**(17), 3607-3618.
22 M. Kaviany, *Springerverlag*, 1995.
23 U. Pasaogullari and C. Y. Wang, *Electrochim Acta*, 2004, **49**(25), 4359-4369.
24 C. Y. Wang and P. Cheng, *Adv Heat Tran*, 1997, **30**, 93-196.
25 U. Pasaogullari and C. Y. Wang, *J Electrochem Soc*, 2004, **151**(3), A399-A406.
26 I. Banerjee, J. M. Modak, K. Bandopadhyay, D. Das and B. R. Maiti, *J Biotechnol*, 2001, **87**(3), 211-223.
27 S. J. Pirt, *Proceedings of the Royal Society of London. Series B, Biological Sciences*, 1965, 224-231.
28 J. Obeid, J. P. Magnin, J. M. Flaus, O. Adrot, J. C. Willison and R. Zlatev, *J Hydrogen Energ*, 2009, **34**(1), 180-185.
29 S. Patankar, *CRC Press*, 1980.
30 I. Akkerman, M. Janssen, J. Rocha, and R. H. Wijffels, *J Hydrogen Energ*, 2002, **27**(11), 1195-1208.